Materials Science & Engineering A 735 (2018) 208–217

Contents lists available at ScienceDirect

Materials Science & Engineering A

journal homepage: www.elsevier.com/locate/msea

Effects of hydrogen and microstructure on tensile properties and failure mechanism of 304L K-TIG welded joint

Xiaogang Li[a,b], Baoming Gong[a,b], Xiuguo Liu[a], Caiyan Deng[a,b,*], Yizhe Li[a,b]

[a] Department of Materials Science and Engineering, Tianjin University, Tianjin 300350, China
[b] Tianjin Key Laboratory of Advanced Joining Technology, Tianjin 300350, China

ARTICLE INFO

Keywords:
Stainless steel
Hydrogen embrittlement
Tensile behaviour
Microstructure
Welding

ABSTRACT

The effects of hydrogen on the mechanical properties of 304L keyhole tungsten inert gas welded joint were investigated in the study. The presence of hydrogen resulted in a significant decrease in the macroscopic ductility of the weld metal, and fracture may be initiated at the sites of clustered dislocations due to hydrogen atoms. Moreover, it is found that hydrogen may result in more severe loss in ductility and noticeable decrease in the flow stress and strength of the base metal, because of the interplay between the hydrogen atoms and strain-induced α′ martensite. Strain-induced α′ martensitic transformation and phase boundaries in the base metal may provide more sites for the accumulation of hydrogen and dislocations, leading to an appreciable decrease in the ductility and strength of the base metal.

1. Introduction

Hydrogen embrittlement refers to the introduction and subsequent diffusion of hydrogen atoms into hydride-forming metals, and it causes degradation of the mechanical properties of metals, eventually leading to fracture. Austenitic stainless steels (ASS) have excellent mechanical properties and corrosion resistance and therefore have been widely used in many industrial applications, including gas and oil storage structures, which are exposed to extreme hydrogen environments [1–6]. The hydrogen embrittlement susceptibility of ASS is strongly determined by many factors, i.e. stability of austenite [7] and incompatibilities of local strain [8]. In particular, α′ martensite is more sensitive to hydrogen than austenite because of its higher hydrogen diffusion coefficient [9], which makes it a “highway” for hydrogen motion [10]. Metastable ASS, such as type 304, are known to undergo strain-induced α′ martensitic transformation during plastic deformation [11–18] and often suffer from severe hydrogen embrittlement. Therefore, the effects of the presence of hydrogen and austenite to α′ martensite phase transformation on the mechanical properties have been widely investigated in both ASS and the related welding joints [19,20]. Moreover, due to the complex heat cycle during welding, the welded joint is heterogeneous in microstructure. The microstructure of the weld metal is usually distinct from that of the base metal [19,21], which may significantly affect hydrogen transport [22]. Olden et al. reported that in the API X70 pipeline steel welded joint the hydrogen diffusion coefficient at room temperature was 7.60×10^{-11} m^2/s for the base metal consisted of banded ferrite-pearlite with traces of martensite, while 4.01×10^{-11} m^2/s for the weld metal composed of grain boundary ferrite, acicular ferrite, polygonal ferrite and some side-plates [22]. Jackson et al. noted that hydrogen led stress concentrations around deformation bands impinging on austenite/ferrite phase boundaries in 304L/308L and 21Cr-6Ni-9Mn/308L austenitic stainless steel fusion welds, which facilitated microcrack nucleation [21]. It was also previously observed by Naumann and Michler that delta ferrite in ASS welds would not raise the susceptibility to hydrogen embrittlement [19]. Keyhole tungsten inert gas (K-TIG) welding is an efficient technique widely applied to ASS, and it can allow for deeper penetration than does the classical TIG method [23]. Although hydrogen embrittlement of ASS and its welded parts has been reported [24–30], little is known about hydrogen embrittlement of ASS K-TIG welded joints. For ASS widely employed in hydrogen-containing environments, the effects of hydrogen on the plasticity and strength of K-TIG welded joints should be critically evaluated.

In the study, the effects of hydrogen on the tensile properties and failure mechanism of the weld metal and base metal in 304L K-TIG welded joints were experimentally investigated. Electrochemical hydrogen charging and subsequent tensile tests were conducted to investigate the loss in plasticity and strength of the weld metal and base metal. The microstructures of the fractured samples were observed by scanning electron microscopy (SEM), electron backscatter diffraction

* Corresponding author at: Department of Materials Science and Engineering, Tianjin University, Tianjin 300350, China.
E-mail address: dengcy@tju.edu.cn (C. Deng).

https://doi.org/10.1016/j.msea.2018.08.045
Received 8 April 2018; Received in revised form 15 August 2018; Accepted 16 August 2018
Available online 17 August 2018
0921-5093/

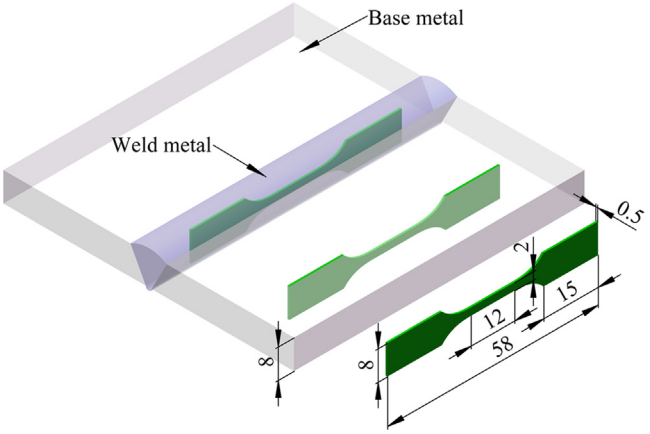

Fig. 1. Dimensions and sampling location of tensile samples (in mm).

(EBSD), and transmission electron microscopy (TEM). The results indicated that the presence of hydrogen decreased the ductility of the weld metal; this was attributed to the interactions between hydrogen and the dislocations. In addition, the base metal suffered severe loss of plasticity and strength because of the austenite to α′ martensite phase transformation caused by the accumulation of hydrogen around the phase boundary.

2. Material and methods

The base metal used in this study was AISI 304L stainless steel. The dimensions of the steel plate were 300 mm × 150 mm × 8 mm. The average chemical composition (in mass percentages) of the base metal was 18.19 Cr, 8.26 Ni, 0.54 Mn, 0.17 Mo, 0.35 Si, 0.16 Co, 0.081 N, 0.033 P, 0.024 S, and 0.019 C (Fe balance). The K-TIG method was used to weld 8-mm-thick 304L stainless-steel plates without the filler metal in a single pass, in a flat position. The welding current, arc voltage and welding speed were 520 A, 16.5 V, and 6 mm/s, respectively. The shielding gas was pure argon, with a flow rate of 35 L/min. The sample was chemically etched using a solution of hydrochloric acid (30 vol%), nitric acid (30 vol%), and acetic acid (40 vol%) and then observed under an optical microscope. The microstructures of the K-TIG welded joint were also examined by EBSD. The sample for EBSD observations was ground to 3000 grit and electropolished using a solution of ethyl alcohol (95 vol%) and perchloric acid (5 vol%) at 30 V for 30 s. The step size for the EBSD operation was 0.1 μm.

The dimensions of the tensile samples are shown in Fig. 1. The tensile samples were grinded down to 2000 grit and then mechanically

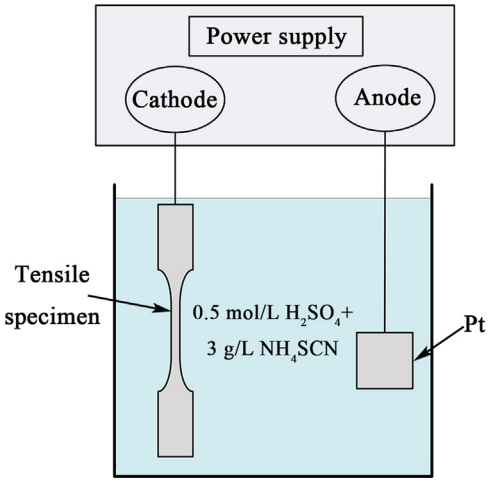

Fig. 2. Schematic of the system used for electrolytic hydrogen charging.

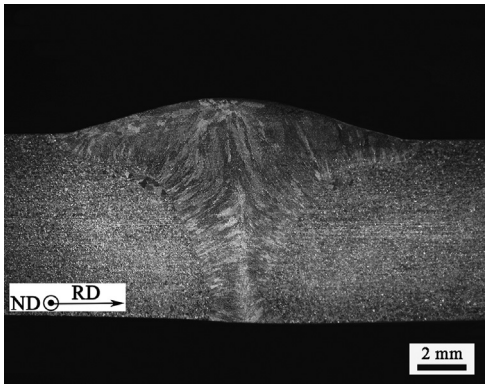

Fig. 3. Optical microscope image of a cross-section of the K-TIG welded joint.

polished down to a 0.25 μm surface finish. The final thickness of sample was 0.5 mm. The polished samples were cathodically charged at 25 °C in 0.5 mol/L H_2SO_4 + 3 g/L NH_4SCN solution under a current density of 80 mA/cm^2 for 48 h to introduce hydrogen, and the samples were completely immersed during the hydrogen charging as shown in Fig. 2.

Tensile tests were conducted immediately after charging, at 25 °C with a strain rate of 2.7×10^{-4} s^{-1}. Under each condition, three samples were repeated to ensure the data reliability. The relative elongation, relative reduction of area, and relative ultimate tensile strength (*UTS*) were used to quantify the losses in the tensile properties under all conditions, as follows:

$$I_\delta(\%) = \frac{\delta_H}{\delta_0} \quad (1)$$

$$I_\psi(\%) = \frac{\psi_H}{\psi_0} \quad (2)$$

$$I_{UTS}(\%) = \frac{UTS_H}{UTS_0} \quad (3)$$

where δ and Ψ are the elongation to failure and reduction in area of the samples, respectively. The subscripts 0 and H denote the pristine and charged samples, respectively. After the tensile tests, the fracture morphologies were investigated by SEM. The deformation

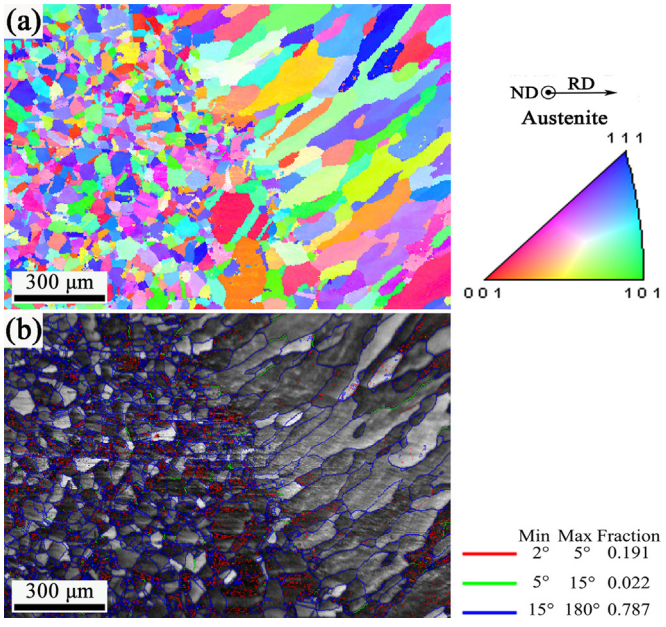

Fig. 4. EBSD images of the fusion zone, heat-affected zone, and base metal of the welded joint: (a) IPF map; (b) misorientation distribution.